

Abnormal Neural Oscillations in Schizophrenia Assessed by Spectral Power Ratio of MEG during Word Processing

Tingting Xu, *Student Member, IEEE*, Massoud Stephane, and Keshab K. Parhi, *Fellow, IEEE*

Abstract— This study investigated spectral power of neural oscillations associated with word processing in schizophrenia. Magnetoencephalography (MEG) data were acquired from 12 schizophrenia patients and 10 healthy controls during a visual word processing task. Two *spectral power ratio* (SPR) feature sets: the *band power ratio* (BPR) and the *window power ratio* (WPR) were extracted from MEG data in 5 frequency bands, 4 time windows of word processing, and at locations covering whole head. Cluster-based nonparametric permutation tests were employed to identify SPRs that show significant between-group difference. Machine learning based feature selection and classification techniques were then employed to select optimal combinations of the significant SPR features, and distinguish schizophrenia patients from healthy controls. We identified 3 BPR clusters and 3 WPR clusters that show significant oscillation power difference between groups. These include the *theta/delta*, *alpha/delta* and *beta/delta* BPRs during *base-to-encode* and *encode time* windows, and the *beta* band WPR from *base to encode* and from *encode to post* windows. Based on 2 WPR and 1 BPR features combined, over 95% cross-validation classification accuracy was achieved using 3 different linear classifiers separately. These features may have potential as quantitative markers that discriminate schizophrenia patients and healthy controls; however, this needs further validation on larger samples.

Index Terms— schizophrenia, magnetoencephalography (MEG), word processing, neural oscillations, spectral power ratio, feature extraction, classification

I. INTRODUCTION

SCHIZOPHRENIA is a chronic, severe and complex mental illness which affects about 1% of the world population age 18 and older [1]. The key symptoms of the disease include hallucinations, delusions, paranoia, social withdrawal, and disorganization of thought and language [1]. Recent theory has suggested that the psychotic phenomena and the cognitive dysfunctions that characterize schizophrenia are due to disruptions of coordinated activity in cortical circuits [2]–[4]. Accordingly, neural oscillations, a fundamental mechanism for enabling coordinated activity during normal

brain functioning, has become a crucial target for investigating the pathophysiology of schizophrenia, as well as the mechanisms of the cognitive deficits and other symptoms of this disease [4]–[6].

Neural oscillations can be assessed by methods that record dynamic brain activity with high temporal resolution, such as electroencephalogram (EEG) and magnetoencephalogram (MEG). Neural oscillations detected by MEG/EEG correspond to the synchronous firing of the pyramidal neurons. The oscillatory frequency reflects the frequency of neural firing, and the power of a frequency reflects the number of pyramidal neurons firing at that frequency [7]. MEG/EEG studies that examined neural oscillations in schizophrenia at different temporal and spatial scales have reported decreased or increased oscillation power in all frequency bands, including *delta* (<4Hz), *theta* (4-8Hz), *alpha* (8-12Hz), *beta* (12-30Hz) and *gamma* (>30Hz) bands (see [8] for review). The specificity of frequency abnormalities may provide key biological markers linking disease mechanism to the clinical dysfunctions in schizophrenia [8]. Furthermore, some recent MEG/EEG studies showed that band power of neural oscillations during both cognitive tasks and resting state could be used as quantitative features to distinguish schizophrenia patients from healthy controls with machine learning classifiers [9]–[15].

In the present study, we use MEG to investigate the spectral power of neural oscillatory activity during word processing in schizophrenia. Studies have shown that cognitive functions modulate neural oscillations at multiple frequencies simultaneously [7], and this modulation takes place at the frequency, spatial, and temporal dimensions [13], [16], [17]. Additionally, schizophrenia could be evolutionarily related to the development of language in homosapiens, and, in fact, language disorder is one of the core symptoms in this illness [18]. Linguistic research in schizophrenia has frequently shown abnormalities at multiple levels of language processing (lexical, semantic, syntactic and pragmatic levels) [19], as well as abnormal dynamic between these processing levels [20]. Therefore, our central hypothesis here is that the spectral power patterns of neural oscillations in schizophrenic patients differ from healthy controls at certain frequency ranges, brain locations and time periods of word processing. Such spectral-spatial-temporal information can be extracted as quantitative features from MEG recordings to distinguish schizophrenia patients from healthy subjects.

T. Xu and K. K. Parhi are with the Department of Electrical and Computer Engineering, University of Minnesota, Minneapolis, MN, 55455, USA (e-mail: xuxxx591@umn.edu, parhi@umn.edu).

M. Stephane was with the Department of Psychiatry, University of Minnesota, and the Brain Science Center, VA Medical Center, Minneapolis, MN, USA. He is now with the Department of Psychiatry, Oregon Health & Science University, Portland, OR, USA. (e-mail: stephane@ohsu.edu).

The key contributions of this work are three-fold. First, we extracted two *spectral power ratio* (SPR) feature sets: the *band power ratio* (BPR) and the *window power ratio* (WPR), to assess neural oscillations in schizophrenia. Spectral power has been employed in previous studies to delineate oscillatory abnormalities in schizophrenia, mostly in the form of *absolute band power* (ABP) [15], [21]–[23] or *relative band power* (RBP), i.e., ABP normalized by the total power [10], [24]. Unlike ABP and RBP, which characterize oscillation power in different frequency bands and in different time windows separately, the BPR and the WPR reflect the inter-relationships of spectral power between different frequency bands, and between different time periods of word processing, respectively. On the one hand, the ratio of band power (BPR) amplifies the increase of power in one band and the decrease of power in another band, which has been shown to be effective in epileptic seizure prediction [25], [26], seizure detection [27], and stroke diagnosis [28]. Previous work has also shown the discriminating power of BPR in schizophrenia classification, using single-trial MEG data during sentence processing [14]. On the other hand, the ratio of power in two consecutive time windows (WPR) for a specified spectral band captures the power change across different time periods of word processing, which could not be assessed by single window based analysis. As such, the BPR and WPR provide information about the frequency and temporal dynamics of neural oscillations, respectively. To the best of our knowledge, BPR and WPR have not been employed together before to analyze MEG data collected from schizophrenia patients during word processing.

Second, we employed cluster-based non-parametric permutation test [29] to identify statistically significant SPR features. SPR features are extracted from hundreds of brain locations measured by MEG. Discriminating features identified by sample-wise uncorrected p -values or other univariate feature ranking methods that measure the between-group difference at single feature level may be false discoveries due to multiple comparisons. Some previous studies employed traditional Bonferroni correction [10], [24] or false discovery rate (FDR) control procedures [22] for multiple comparison correction. These methods are not optimized for MEG data, and may lead to high false negative rate (FNR), i.e., low sensitivity for detecting significant features, due to the small sample size compared with the large feature size. The cluster-based non-parametric permutation tests [29] we employed in this study control the FDR while maintaining a low FNR, which results in high specificity and sensitivity of the discriminating features. It may be noted that cluster-based non-parametric permutation test has rarely been employed as a feature selection procedure in the context of schizophrenia classification.

Third, after identifying statistically significant SPR features, we applied machine learning based feature selection algorithm to select optimal feature combinations for classifying schizophrenia patients from healthy controls. We achieved over 95% classification accuracy using three different linear classifiers separately, following cross validation procedures.

The rest of the paper is organized as follows. Section II describes the details of the MEG data acquisition, SPR feature

extraction, statistical testing and classification procedures. Sections III and IV presents the data analysis results and discusses the significance and limitations of the work, respectively. Section V concludes the current work and points out future directions.

II. METHODS

A. Subjects

Participants included 12 schizophrenia patients (12 male) and 10 healthy controls (9 male). All the subjects were native English speakers and were right-handed. Handedness was assessed by the Edinburgh Handedness Inventory [30]. None of the control subjects had neurological disease or major medical illness. All the patients met the criteria of the “Diagnostic and Statistical Manual of Mental Disorders, 4th Edition (DSM-IV) [31]” for schizophrenia or schizoaffective disorder. All the subjects gave written informed consent before entering the study. The experimental protocol was approved by the relevant Institutional Review Boards.

Measures of premorbid intellectual functioning were obtained using the National Adult Reading Test (NART) [32]. The severity of psychopathology was assessed with the Brief Psychiatric Rating Scale (BPRS) [33] and the Positive and Negative Symptoms Scale (PANSS) [34]. The duration of illness was derived from reviews of patient records. Table I summarizes the demographic and clinical characteristics of the subjects.

TABLE I
DEMOGRAPHIC AND CLINICAL CHARACTERISTICS OF THE SUBJECTS

Characteristics	Control	Patient
	mean (std.)	mean (std.)
Age, year	49.7 (11.1)	49.5 (7.0)
Education, year	15.0 (2.2)	15.5 (4.7)
Parents education, year	13.6 (2.4)	12.4 (2.7)
NART full score	111.3 (7.3)	106.5 (6.8)
NART performance score	110.5 (3.9)	108.0 (3.6)
NART verbal score	109.3 (8.5)	104.4 (7.8)
BPRS	-	41.4 (9.4)
PANSS, negative symptoms	-	7.5 (4.3)
PANSS, positive symptoms	-	8.8 (5.7)
Duration of illness, year	-	22.1 (10.0)
Chlorpromazine equivalent dose, mg	-	330.3 (118.7)

NART: National Adult Reading Test; BPRS: Brief Psychiatric Rating Scale; PANSS = Positive and Negative Syndrome Scale

B. Word Processing Task

Subjects were instructed to distinguish between correct and incorrect word stimuli. A correct stimulus is a set of five real English words, e.g., “cabin-fire-rope-big-the”. An incorrect stimulus is a set of five elements with four real English words and one pronounceable non-word, e.g., “cabin-freet-rope-big-the”. The elements in each stimulus were presented visually one at a time in the center of a monitor placed in front of the subjects. Each element appeared for 750 milliseconds followed by a 250 milliseconds blank screen.

There was a 10-second interval between different trials. Subjects were instructed to read the stimuli silently and press a button with their right index finger for incorrect stimuli.

This word processing task was part of a comprehensive procedure for language evaluation described in detail in previous work [19], [20]. The task is based on a standard psycholinguistic procedure - anomaly detection [35]. Here, the detection of a pronounceable non-English word would require the correct identification - and accordingly processing - of English words. To maximize word processing operations, the task was designed in a way that minimize significantly verbal working memory load. That is, subjects were only required to detect the anomaly (non-English word) and were not required to remember the English words. As there was only one possible anomaly per stimulus, there was a working memory load of one item - the lowest working memory load possible.

In the task, each subject performed 60 trials that included 45 correct stimuli and 15 incorrect stimuli. The average correct response rate was 94.17% for the control group and 87.5% for the patient group. In this study, we only analyze trials with correct stimuli, as we are interested in investigating the abnormal neural oscillation patterns in schizophrenia during normal word processing.

C. MEG Data Acquisition and Preprocessing

During the task, MEG data were recorded from 248 axial gradiometers (Magnes 3600WH, 4-D Neuroimaging, San Diego, CA) in a 2-layer mu-metal magnetically shielded room (IMEDCO, Hagendorf, Switzerland), with a sampling rate of 1024Hz. Subjects were in a supine position with their heads in the sensor helmet and on a head support to minimize movement. Ambient and distant biological magnetic noises were reduced by using 23 SQUID reference channels, which were situated within the sensor and above the cortical channels. Electrooculogram (EOG) and electrocardiogram (ECG) were recorded to identify and correct epochs contaminated by eye movements and heartbeats. Artifacts (blinks and heartbeats) correction was carried out according to an algorithm described by Ille et al [36]. Visual inspection was performed to reject trials with residual artifacts. After preprocessing, successful trials for each subject were down-sampled to 256Hz and averaged across trials for further analysis. Out of the 45 trials with correct stimuli, the number of artifact free trials with correct stimuli did not differ significantly between schizophrenia patients (mean 36, std. 7.2) and controls (mean 41, std. 3.3), p -value > 0.05 .

D. Feature Extraction

The BPR and the WPR feature sets are extracted from the *power spectral density* (PSD) of the MEG recordings. Both BPR and WPR are spatial-temporal-spectral feature sets with each single feature containing specific frequency, time and space information. Details of the feature extraction procedures are described below.

Define Spatial Locations:

Unlike most EEG/MEG studies that extract features from each single MEG sensor separately, we averaged MEG signals

from 3 adjacent sensors before feature extraction. More specifically, for each MEG sensor, we form 8 triangles from its 8 nearest neighbor sensors which have shortest circumference, as shown in Fig. 1. This procedure results in 822 averaged MEG signals for each subject. The spatial location of the averaged signal is defined as the geometric center of the 3 averaged MEG sensors.

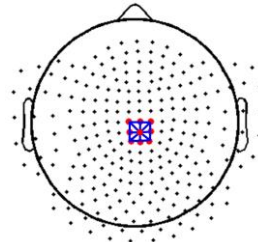


Fig. 1. Average MEG signals from three adjacent sensors that form a triangle with shortest circumference

The reason for averaging signals from adjacent sensors is that MEG recordings are generally considered “noisy” where the noise level is higher than the signal of interest. To cope with this problem, after averaging trials from same MEG sensor, we average signals from adjacent sensors to further suppress the random noise components. In addition, due to volume conduction effect, MEG gradiometers tend to show spread activation in sensor space. That is, MEG sensors that are close to each other tend to record similar activities, which make it reasonable to average signals from a few adjacent sensors. Furthermore, with axial gradiometers, a local brain source is best captured by adjacent sensors, rather than by a sensor just above the source [11].

Define Time Windows:

The averaged MEG signal from each spatial location is further segmented into 5 phases of word processing, using time windows shown in Fig. 2: 1) *baseline* (BA), three seconds right before the onset of the first word; 2) *transition from baseline to encoding* (BE), one second before and two seconds after the onset of the first word; 3) *encoding* (EN), stimuli presentation, five seconds right after the onset of the first word; 4) *transition from encoding to post-stimuli* (EP), one second before the end of stimuli presentation to two seconds after stimuli presentation; 5) *post-stimuli* (PO), three seconds right after stimuli presentation. After this step, new MEG segments are obtained with each one corresponding to one spatial location and one time window (phase of word processing).

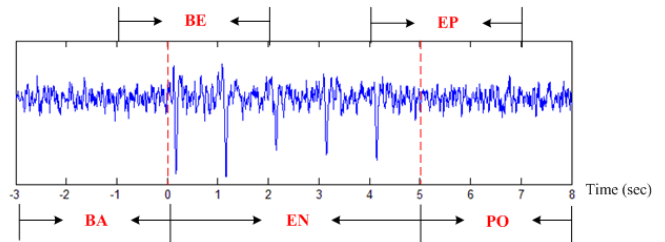


Fig. 2. Segmentation of the MEG signal into 5 time windows of word processing: 1) *baseline* (BA), 2) *transition from baseline to encoding* (BE), 3) *encoding* (EN), 4) *transition from encoding to post-stimuli* (EP), and 5) *post-stimuli* (PO).

Define Spectral Power Ratios:

For each MEG segment, the PSD, which describes how the power of a signal is distributed over different frequencies, is estimated using the Welch algorithm [37], which can be computed in an efficient manner with low complexity [38]. Afterwards, the spectral power is computed in 5 frequency bands by integrating the PSD within that frequency band. The frequency ranges of the 5 bands of interests are: *delta* (1-4Hz), *theta* (4-8Hz), *alpha* (8-13 Hz), *beta* (13-30Hz) and *gamma* (30-57 Hz). The spectral power of MEG signal at the i^{th} spatial location, the j^{th} time window, and the k^{th} frequency band is defined as:

$$P_{i,j,k} = \sum_{f \in [f_{\min}^k, f_{\max}^k]} PSD_{i,j,k}(f), \quad (1)$$

$$i = 1, \dots, 822; j = 1, \dots, 5; k = 1, \dots, 5.$$

where f_{\min}^k and f_{\max}^k represent the lowest and highest frequency of the k^{th} frequency band, respectively.

The first SPR feature set BPR is defined as the ratio of spectral power between two different frequency bands, at the same spatial location and in the same time window. The BPR between band k_1 and band k_2 , at region i and during time window j is defined as:

$$BPR_{i,j,k_1,k_2} = P_{i,j,k_1} / P_{i,j,k_2}, \quad i = 1, \dots, 822; \quad (2)$$

$$j = 2, \dots, 5; k_1, k_2 = 1, \dots, 5; k_1 > k_2.$$

The second SPR feature set WPR is defined as the percentage power change across two consecutive time windows. The WPR between the j^{th} and the $(j-1)^{th}$ time window, at the k^{th} frequency band and the i^{th} region is defined as:

$$WPR_{i,j,k} = (P_{i,j,k} - P_{i,j-1,k}) / P_{i,j-1,k}, \quad (3)$$

$$i = 1, \dots, 822; j = 2, \dots, 5; k = 1, \dots, 5.$$

The total number of BPR features is 10 BPRs * 4 time windows * 822 spatial locations = 32880 (BA window is not used). The total number of WPR features is: 4 WPRs * 5 frequency bands * 822 spatial locations = 16440. All features are normalized to have zero mean and standard deviation before further analysis.

E. Statistical Testing

Non-parametric Permutation test is employed to determine the statistical significance of the extracted SPR features and control the false positive rate (Type I error) caused by multiple comparisons [29]. It is performed for BPR in each time window and WPR in each frequency bands separately. The permutation test uses a test statistic that is based on clustering of adjacent spatial locations that exhibit a similar SPR difference (in sign and magnitude) between patient group and control group. The calculation of the test statistic involves the following steps:

Step 1: Compute the t -score for each SPR feature from all spatial locations: $t = (\bar{X}_c - \bar{X}_p) / \sqrt{s_c^2 / N_c + s_p^2 / N_p}$, where

\bar{X}_c and \bar{X}_p are the sample means, s_c and s_p are the sample standard deviations, and N_c and N_p are the sample sizes of the control group and the patient group, respectively. This t -score is called the sample-specific uncorrected t -score.

Step 2: Select all SPRs with absolute value of uncorrected t -score greater than a threshold, 2.5 in the current study. This step identifies a set of "candidate positives", of which a high proportion is likely to be true.

Step 3: Cluster the selected features in connected sets based on spatial adjacency. In this study, we define two spatial locations as neighbors if their distance is less than 0.03 mm. Note that the clustering is performed for features with positive and negative t -scores separately.

Step 4: The cluster-level statistics is defined as the sum of t -scores within a cluster.

After getting the cluster-level test statistics for all clusters, the significance of these clusters is obtained by calculating the Monte-Carlo estimate of the p -values. The steps are as follows:

Step 1: Randomly reassign the group identity of each subject without replacement.

Step 2: Calculate the cluster-level test statistics on this random partition and take the largest of these statistics.

Step 3: Repeat step 1 and step 2 for a large number of times, 50,000 in this study, and construct a permutation distribution of the test statistics.

Step 4: The Monte Carlo p -value of a cluster is defined as the proportion of random partitions that have a larger test statistic than the observed one. An SPR cluster with Monte Carlo p -value less than 0.05 is considered statistically significant in this study.

F. Feature Selection and Classification

After identifying statistically significant SPRs, we test whether they could be used as features in machine learning classifiers to distinguish schizophrenia patients from healthy controls (predict diagnosis) with high accuracy. The mean SPR within a significant cluster is used as a scalar feature representing the cluster. A feature ranking algorithm based on the *minimum redundancy and maximum relevance* (mRMR) criteria is employed to select the optimal feature combinations for classification [39]. Since our sample size is small, to avoid complex classification models overfitting the data, three commonly used linear classifiers are employed to classify patients vs. controls: *linear discriminant analysis* (LDA) [40], *perceptron* [41] and *linear support vector machine* (SVM) [42], [43]. We employed a cross-validation scheme to test the generalization ability of the classification results. Three controls and four patients are randomly chosen from each group to form a testing set. The rest seven controls and eight patients are used as training set to train the classifiers. We construct 1000 such training and testing sets by random sampling, and calculate the average classification accuracy, specificity and sensitivity of each classifier over the 1000 test sets.

III. RESULTS

A. Significant BPR Features

Each SPR feature contains specific frequency, time and space information. In Fig. 3, we show the frequency-time distribution of the BPR features with absolute value of uncorrected t -score greater than 2.5. Most of the BPR features that show significant between group difference before the permutation test are: 1) BPR ($theta/delta$, EN), i.e., the $theta/delta$ band power ratio during the *encode* window, 2) BPR ($alpha/delta$, BE), i.e., the $alpha/delta$ band power ratio during the *base-to-encode* window, and 3) BPR ($beta/delta$, EN), i.e., the $beta/delta$ band power ratio during the *encode* window. The spatial locations of these three significant BPRs are shown in Fig. 4.

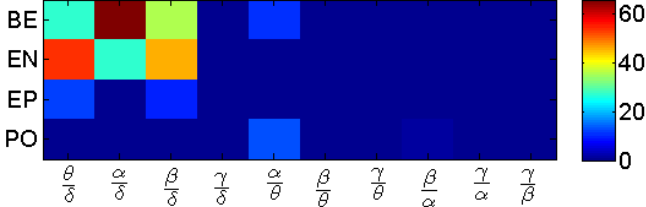


Fig. 3. Number of occurrences of each BPR that show significant between group differences (absolute value of uncorrected t -score > 2.5) in each time window

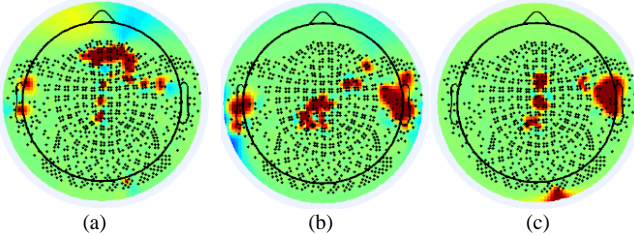


Fig. 4. Spatial locations of BPR features with absolute value of uncorrected t -score > 2.5 for (a) BPR ($theta/delta$, EN), (b) BPR ($alpha/delta$, BE), and (c) BPR ($beta/delta$, EN)

From Fig. 4, we can observe several spatial clusters associate with each of the three significant BPRs. The significant BPR ($theta/delta$, EN) features are located at the middle to right frontal, left-temporal and middle parietal areas. The significant BPR ($alpha/delta$, BE) features are located at the left temporal, middle parietal, right temporal and right frontal areas. The significant BPR ($beta/delta$, EN) features are located at the middle frontal-parietal, right temporal and occipital areas. However, only three clusters of these features pass the permutation test (corrected p -value < 0.05), including 1) the middle to right frontal cluster of BPR ($theta/delta$, EN), average t -score = -2.792, corrected p -value = 0.024, 2) the middle parietal cluster of BPR ($alpha/delta$, BE), average t -score = -2.798, corrected p -value = 0.047, and 3) the middle frontal-parietal cluster of BPR ($beta/delta$, EN), average t -score = -2.770, corrected p -value = 0.046. The 3D head plot of the spatial locations, the boxplot of the mean SPR within cluster, and the normalized PSD of a signal in the cluster are shown in Figs. 5, 6 and 7, for the three significant clusters, respectively.

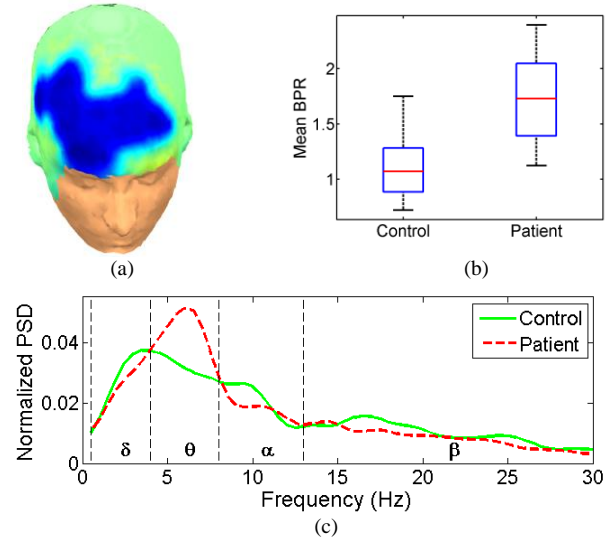


Fig. 5. (a) Spatial locations (middle to right frontal areas) that show significantly increased BPR ($theta/delta$, EN) in schizophrenia patients (average t -score = -2.792, corrected p -value = 0.024). (b) Boxplot of the mean BPR within cluster. (c) Normalized PSD of MEG signal from a location in the cluster for control group and patient group.

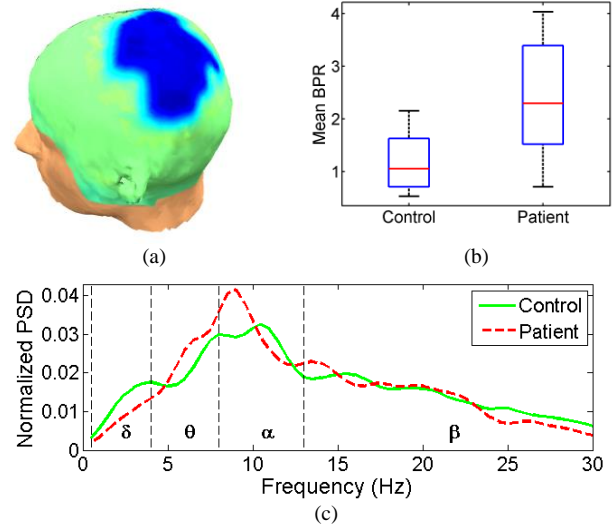


Fig. 6. (a) Spatial locations (middle parietal area) that show significantly increased BPR ($alpha/delta$, BE) in schizophrenia patients (average t -score = -2.798, corrected p -value = 0.047). (b) Boxplot of the mean BPR within cluster. (c) Normalized PSD of MEG signal from a location in the cluster for control group and patient group.

From Fig. 5, we can see that patient group shows significantly increased $theta/delta$ BPR during encoding period of word processing, at the middle to right frontal area. This is due to a decreased proportion of $delta$ band power and an increased proportion of $theta$ band power in the full spectrum in patient group. In Fig. 6, we can observe that patients show an increased $alpha/delta$ power ratio at the middle parietal area during baseline to encoding period of word processing. The PSD plot shows that the proportion of $delta$ power decreases and the proportion of $alpha$ power increases in schizophrenia patients. Fig. 7 shows an increased $beta/delta$ power ratio at the

middle frontal-parietal areas, during encoding phase of word processing. This is due to a decreased portion of *delta* band power and an increased proportion of *beta* band power in the full spectrum of the MEG signal in patient group, as shown in the PSD plot.

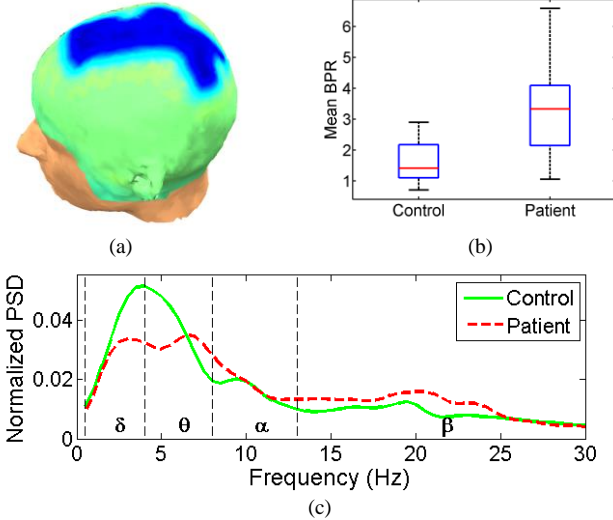


Fig. 7. (a) Spatial locations (middle frontal-parietal areas) that show significantly increased BPR (*beta/delta*, EN) in schizophrenia patients (average t -score = -2.770, corrected p -value = 0.046). (b) Boxplot of the mean BPR within cluster. (c) Normalized PSD of MEG signal from a location in the cluster for control group and patient group.

B. Significant WPR Features

Similarly to the BPR features, in Fig. 8, we show the time-frequency distribution of all WPRs with absolute value of uncorrected t -score greater than 2.5. Most of the WPR features that show significant between-group difference before permutation tests are the WPR (BE/BA, *beta*), i.e., the *beta* band power ratio across *baseline* and *base-to-encode* time windows, and the WPR (PO/EP, *beta*), i.e., the *beta* band power ratio across *encode-to-post* and *post-encoding* time windows. The spatial locations of the two WPRs are shown in Fig. 9.

From Fig. 9, we can observe that the significant WPR (BE/BA, *beta*) features are mainly located at the left parietal and right occipital areas. The significant WPR (PO/EP, *beta*) features are located at the middle frontal, left parietal, right parietal and occipital areas. Among these features, three spatial clusters pass the permutation tests (corrected p -value < 0.05), including 1) the left parietal cluster of the WPR (BE/BA, *beta*), average t -score = 3.015, corrected p -value = 0.037, 2) the right occipital clusters of the WPR (BE/BA, *beta*), average t -score = -3.431, corrected p -value = 0.037, and 3) the middle frontal cluster of the WPR (PO/EP, *beta*), average t -score = -3.115, corrected p -value = 0.013. The 3D head plot of the spatial locations, the boxplot of the mean WPR within cluster, and the *beta* band spectrogram of a signal in the cluster for each group are shown in Figs. 10 to 12, for the three significant WPR clusters, respectively.

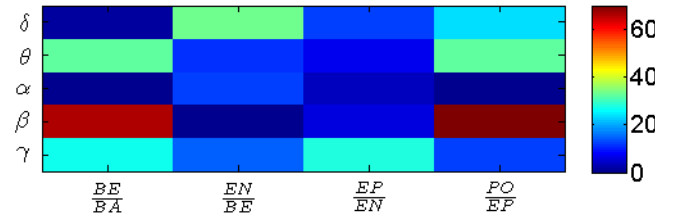


Fig. 8. Number of occurrence of each WPR in different frequency bands with absolute value of uncorrected t -score > 2.5

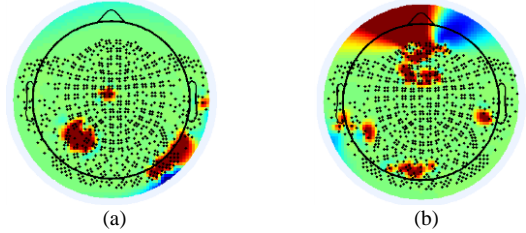


Fig. 9. Spatial locations of WPR features with absolute value of uncorrected t -score > 2.5 for: (a) WPR (BE/BA, *beta*), (b) WPR (PO/EP, *beta*)

Fig. 10 shows a decreased WPR (BE/BA, *beta*) at the right occipital area in patients. From the spectrogram, we can see that from the BA to BE phase of word processing, control group shows a significantly increased *beta* band power while opposite change is observed in patient group. Therefore the WPR (BE/BA, *beta*) is lower in patient group compared with that in control group. Fig. 11 shows a significantly increased WPR (BE/BA, *beta*) at the left parietal area in schizophrenia patients. This is due to an increase of *beta* band power from BA to BE window in patient group, which is not shown in the control group. Fig. 12 shows a significantly increased WPR (PO/PE, *beta*) at the middle frontal area in patient group. This is due to an increase of *beta* band power from EP to PO period in the patient group, as shown in the spectrogram. This increase is not observed in the control group.

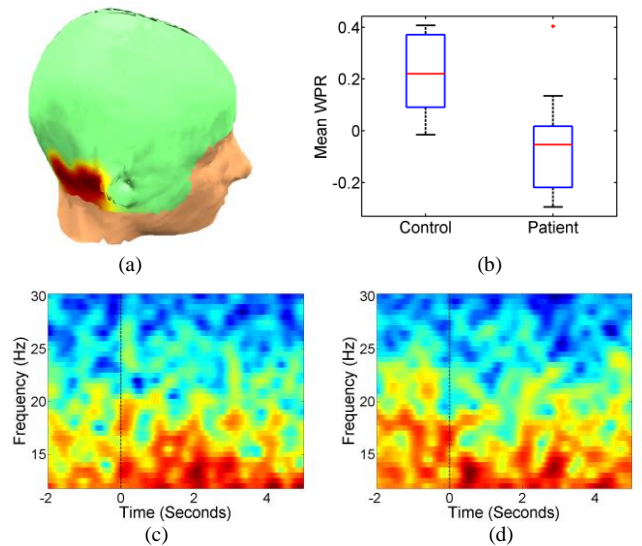


Fig. 10. (a) Spatial locations (right occipital area) that show significantly decreased WPR (BE/BA, *beta*) in schizophrenia patients (average t -score = 3.015, corrected p -value = 0.037). (b) Boxplot of the mean WPR within cluster. (c), (d) Beta band spectrogram of MEG signal from a location in the cluster for control group and patient group, respectively.

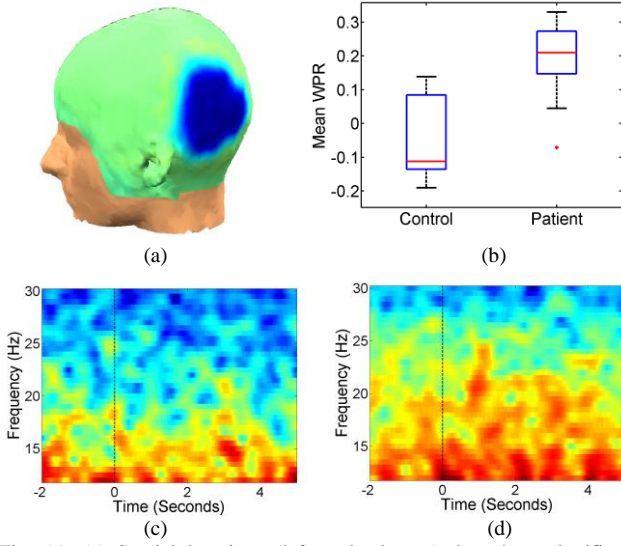


Fig. 11. (a) Spatial locations (left parietal area) that show significantly increased WPR (BE/BA, β) in schizophrenia patients (average t -score = -3.431, corrected p -value = 0.037). (b) Boxplot of the mean WPR within cluster. (c), (d) Beta band spectrogram of MEG signal from a location in the cluster for control group and patient group, respectively.

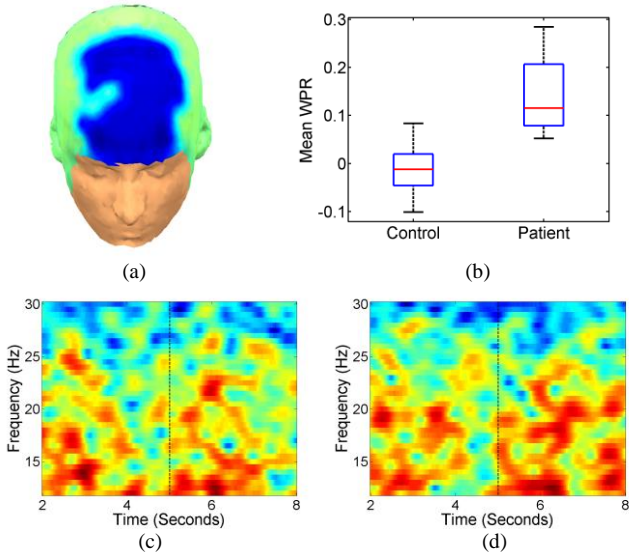


Fig. 12. (a) Spatial locations (middle frontal area) that show significantly increased WPR (PO/EP, β) in schizophrenia patients (average t -score = -3.115, corrected p -value = 0.013). (b) Boxplot of the mean WPR within cluster. (c), (d) Beta band spectrogram of MEG signal from a location in the cluster for control group and patient group, respectively.

C. Classification Results

Table II summarizes the 6 significant SPR clusters. The mean SPR within each cluster is used as a scalar feature and the mRMR algorithm is employed to select combinations of 1 to 6 SPR features for classification. Fig. 13 shows the classification results using combinations of BPR and WPR features, with LDA, perceptron and linear SVM classifiers. The highest classification accuracy is achieved using 2 WPR and 1 BPR features combined for all three classifiers. The three features selected by the mRMR feature ranking algorithm are: F1: WPR (BE/BA, β), F2: BPR (θ/δ , EN), and F3: WPR (PO/EP, β). The detailed classification accuracy, specificity

and sensitivity using these three features are listed in Table III. As comparisons, we also list the classification results using 3 BPR features alone and using 3 WPR features alone in Tables IV and V, respectively. We can see that a combination of BPR and WPR features achieves better classification results than using same number of BPR or WPR features separately.

TABLE II
LIST OF THE 6 SIGNIFICANT SPRs WITH THE CORRESPONDING SPATIAL LOCATIONS, THE MEAN t -SCORE WITHIN CLUSTER, AND THE MONTE CARLO CORRECTED P -VALUE

Feature	Spatial Location	t -score	p -val.
BPR (θ/δ , EN)	middle to right frontal	-2.792	0.024
BPR (α/δ , BE)	middle parietal	-2.798	0.047
BPR (β/δ , EN)	middle frontal-parietal	-2.770	0.046
WPR (BE/BA, β)	right occipital	3.015	0.037
WPR (BE/BA, β)	left parietal	-3.431	0.037
WPR (PO/EP, β)	middle frontal	-3.115	0.013

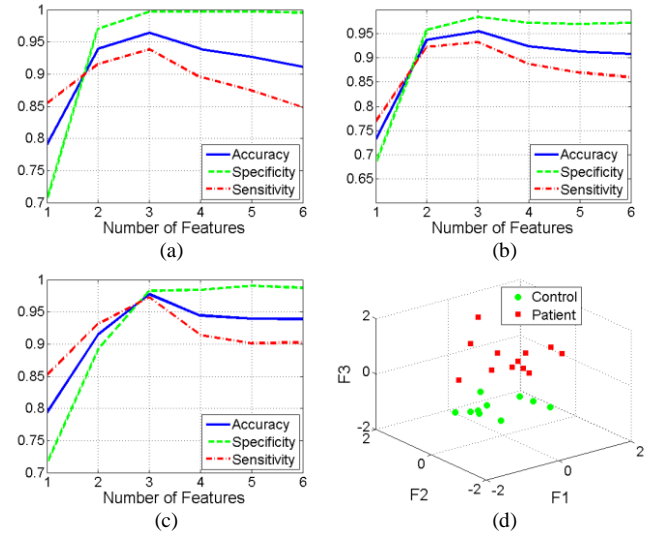


Fig. 13. Classification results using combinations of BPR and WPR features selected by the mRMR algorithm for (a) LDA, (b) perceptron, and (c) linear SVM classifiers. (d) Scatter plot of the 22 subjects in the 3D space formed by top 3 features selected by mRMR algorithm. F1: WPR (BE/BA, β), F2: BPR (θ/δ , EN), F3: WPR (PO/EP, β).

TABLE III
CLASSIFICATION RESULTS USING 1 BPR AND 2 WPR FEATURES SELECTED BY THE MRMR ALGORITHM

Classifier	Accuracy	Specificity	Sensitivity
LDA	0.9637	0.9970	0.9387
Perceptron	0.9550	0.9850	0.9325
Linear SVM	0.9773	0.9830	0.9730

TABLE IV
CLASSIFICATION RESULTS USING 3 BPR FEATURES

Classifier	Accuracy	Specificity	Sensitivity
LDA	0.8097	0.8473	0.7815
Perceptron	0.7354	0.8237	0.6693
Linear SVM	0.7883	0.8060	0.775

TABLE V
CLASSIFICATION RESULTS USING 3 WPR FEATURES

Classifier	Accuracy	Specificity	Sensitivity
LDA	0.9251	0.9897	0.8768
Perceptron	0.8920	0.9420	0.8545
Linear SVM	0.9224	0.9883	0.8730

IV. DISCUSSIONS

Increasing evidence have suggested that abnormalities in the neural oscillatory activity are related to the impairments in various cognitive functions in schizophrenia [4]. In this study, we investigate abnormal neural oscillations in schizophrenia using MEG data from a visual word processing task. Abnormal neural oscillations during cognitive tasks with language stimuli have been reported in both low and high frequency bands, at different brain areas, and during different time periods of language processing [11], [13], [44]. This motivates us to explore spectral-spatial-temporal MEG features to characterize oscillatory activity in frequency, space and time dimensions.

Different from commonly used band power features, which consider different frequency bands or time windows separately, we extracted two SPR feature sets which reflect the relationship of oscillation power between two frequency bands (BPR), and the oscillation power changes across two consecutive time windows of word processing (WPR). The reason for taking ratios of spectral power from two frequency bands is that changes in the power of oscillations occurs at multiple frequencies simultaneously, and patients may show different power changes (increase or decrease) in different frequency bands, compared with healthy controls. Taking ratio between one band that has an increased power and a band that has a decreased power, will further amplify the between-group difference, and thus improve the discriminating power of the feature. Similarly, the oscillation power is changing during different time periods of word processing. Taking the relative power changes across consecutive time windows can reveal the changes of oscillation power across different time periods of word processing, which cannot be learned by analyzing the power in one time window at a time.

After extracting the BPR and the WPR feature sets from 822 spatial locations, 4 time windows of word processing and 5 frequency bands, appropriate statistical tests are needed to identify features that show significant differences between groups. Due to large number of statistical comparisons (822 spatial locations) for each SPR feature, it is not possible to control the family-wise error rate while maintaining low false negative rate, by means of traditional Bonferroni correction or FDR control procedures. Therefore, we employed cluster-based non-parametric permutation test to identify significant SPRs, which controls the false positive rate unconditionally and solve the multiple comparison problem (MCP) in a simple way [29]. The rationale for cluster-based MCP control is based on the idea that MEG signal at a particular location is produced by physiological sources that also affect the MEG from nearby locations. Thus, if a sensor specific null hypothesis is false for

one sensor, then it is also false for the nearby sensors [29].

Note that the cluster-based statistic depends on the threshold that is used to select samples for clustering. It has been shown that the threshold does not affects the false alarm rate of the statistical test but affect the sensitivity of the test [29]. There is no definite criterion about how to choose this threshold to obtain maximum sensitivity for the unknown effect that is present in the data: for a weak and widespread effect, the threshold should be low, and for a strong and localized effect, the threshold should be high [29]. The threshold 2.5 we use in this study is a reasonable sample-specific t -value threshold which corresponds to uncorrected p -value of about 0.025. In addition, we need to point out that the sensitivity and the false negative rate of the cluster-based nonparametric test is less than that of the uncorrected p -value approach which does not control the false discovery rate. This is because multiple testing adjustments control false positives at the potential expense of more false negatives. For example, some features within the right-temporal cluster of the BPR (α/δ , BE) (Fig. 4b) have very high sample-specific uncorrected t -scores. However, the cluster where these features are located did not survive from the MCP correction (marginally, corrected p -value = 0.06). The cluster-based nonparametric tests trade in some sensitivity for false positive rate control to deal with the MCP.

By applying the cluster based permutation test, we identified three BPR clusters which show significantly increased θ/δ , α/δ and β/δ band power ratios during BE and EN periods of word processing, mainly at the frontal-parietal lobes. We also identified three significant WPR clusters which show altered β band power changes when transferring from BA to BE window at the occipital and parietal lobes, and from EP to PO window at the frontal lobe. The spatial locations of the significant SPRs are not restricted to one specific cortical area but rather involved several different brain regions. This finding supports recent theory that the cognitive dysfunctions that characterize schizophrenia are not due to a circumscribed deficit but rather represent a distributed impairment involving many cortical areas and their connectivity [4]. According to our results, the most impaired regions are the frontal-parietal areas. Dysconnections of the frontal-parietal networks have been shown to contribute to cognitive impairment in schizophrenia [45]. Previous studies have also reported abnormalities in these areas in word processing and verbal working memory tasks [11], [13], [44]. The frequency distribution of the significant SPRs show that abnormal oscillations occur in all frequency bands, which is consistent with previous findings [8]. Furthermore, the time periods when these abnormalities occur include the baseline to encoding phase of word processing, as well as the post-encoding periods. These findings suggest failure of the neural systems to respond to task and problem to resume idle state after task, which is consistent with previous findings using event-related-desynchronization/synchronization (ERD / ERS) features [13].

Finally, based on combination of two WPR and one BPR features, over 95% cross validation classification accuracy can be achieved using three different linear classifiers separately.

This result is better than using same number of BPR or WPR features separately, since WPR and BPR offer complementary information to each other. And the mRMR feature selection algorithm selects the optimal feature combinations that maximize the relevant information for classification, while minimizing the redundant information among features [39]. A number of recent studies have also reported schizophrenia classification results using various types of EEG/MEG features and classification methods, as listed in Table VI. The promising result of this study suggests high discriminating power of the identified SPR features, as well as the effectiveness of the feature extraction and selection methods. The reader is, however, cautioned that the present classification results are based on a small sample size (12 patients vs. 10 controls) and have not been fully validated on large samples. To note, only linear classifiers are employed in this study in order to avoid overfitting the data with small sample size. More complex classification models can be designed in future studies with a larger sample size.

A limitation of the current study is that the spatial resolution of the significant SPRs is relatively low. This is due to the spatial resolution of the imaging modality as well as the cluster-based statistical testing procedure. Source localization techniques can be used in future studies to obtain better localization of the significant SPR features. Besides, as mentioned above, the results of the study are limited by small sample size. Therefore, the main purpose of the study is to provide new ways of extracting and identifying discriminating neural oscillation patterns. The findings should be viewed as exploratory and need to be validated in future study with large samples.

V. CONCLUSIONS

In summary, this study analyzed abnormal neural oscillatory activity in schizophrenia patients during visual word processing

task. Two spectral-spatial-temporal feature sets: the BPR and the WPR were extracted from MEG recordings as quantitative features. Cluster-based nonparametric permutation tests identified 3 BPR clusters and 3 WPR clusters that show significant differences between schizophrenia patients and healthy controls. Using 2 WPR features and 1 BPR feature combined, over 95% cross validation accuracy was achieved in classifying 12 patients from 10 controls, using LDA, perceptron and linear SVM classifiers separately. Future work will be directed towards exploring more effective features from neural oscillations using neuroimaging, signal processing and machine learning techniques, and to test the robustness of the proposed scheme on other datasets. More detailed feature analysis such as source localization will also be performed to find more accurate spatial locations of the key features.

VI. ACKNOWLEDGEMENT

The authors are grateful to the anonymous reviewers for their constructive comments. The research was supported in part by an Interdisciplinary Doctoral Fellowship and a Doctoral Dissertation Fellowship from the University of Minnesota graduate school.

REFERENCES

- [1] "NIMH · Schizophrenia." [Online]. Available: <http://www.nimh.nih.gov/health/topics/schizophrenia/index.shtml>. [Accessed: 23-Sep-2014].
- [2] W. A. Phillips and S. M. Silverstein, "Convergence of biological and psychological perspectives on cognitive coordination in schizophrenia.," *Behav. Brain Sci.*, vol. 26, no. 1, pp. 65–82; discussion 82–137, 2003.
- [3] K. J. Friston and K. J. Friston, "Schizophrenia and the disconnection hypothesis.," *Acta Psychiatr. Scand. Suppl.*, vol. 395, pp. 68–79, 1999.
- [4] P. J. Uhlhaas and W. Singer, "Abnormal neural oscillations and synchrony in schizophrenia.," *Nat. Rev. Neurosci.*, vol. 11, pp. 100–113, 2010.
- [5] G. Buzsáki and A. Draguhn, "Neuronal oscillations in cortical

TABLE VI
SUMMARY OF RECENT EEG/MEG CLASSIFICATION STUDIES FOR SCHIZOPHRENIA IDENTIFICATION

Study	Task	Signal	Feature	Feature Selection	Classifier	Nc/Np	Accuracy
Boostani et al. (2009) [9]	rest, eyes open	EEG	AR coefficients, band power, fractal dimension	no	boosted LDA	18/13	87.51%
Sabeti et al. (2009) [46]	rest, eyes open	EEG	entropy, complexity	genetic programming	LDA, Adaboost	20/20	89%, 91%
Sabeti et al. (2011) [15]	rest, eyes open	EEG	AR coefficients, band power, fractal dimension	mutual information, genetic programming	LDA, Adaboost	20/20	85.9% 91.94%
Escudero et al. (2013) [10]	rest	MEG	frequency spectrum	correlation based	logistic regression	17/15	71.3%
Ince et al. (2009) [11]	working memory	MEG	ERD/ERS	AUC	LDA	23/15	83.8%~94.6%
Xu et al. (2013) [13]	word processing	MEG	ERD/ERS	Fscore, SVM-RFE	linear SVM	10/12	90.91%
Present work	word processing	MEG	BPR, WPR	non-parametric permutation test mRMR	LDA perceptron linear SVM	10/12	96.37% 95.50% 97.73%

Nc/Np = number of controls/number of patients; AR = auto-regressive; ERD/ERS = event related desynchronization/synchronization; ANN = artificial neural network; LDA = linear discriminant analysis; SVM = support vector machine; AUC = area under curve

- networks.," *Science*, vol. 304, no. 5679, pp. 1926–1929, 2004.
- [6] G. Buzsáki, *Rhythms of the Brain*, vol. 1, 2006.
- [7] G. Pfurtscheller and F. H. Lopes da Silva, "Functional meaning of even-related desynchronization (ERD) and synchronization (ERS)," in *Event-Related Desynchronization: Handbook of Electroencephalography and Clinical Neurophysiology*, 1999, pp. 51–65.
- [8] L. V. Moran and L. E. Hong, "High vs low frequency neural oscillations in schizophrenia," *Schizophrenia Bulletin*, vol. 37, no. 4, pp. 659–663, 2011.
- [9] R. Boostani, K. Sadatnezhad, and M. Sabeti, "An efficient classifier to diagnose of schizophrenia based on the EEG signals," *Expert Syst. Appl.*, vol. 36, pp. 6492–6499, 2009.
- [10] J. Escudero, E. Ifeachor, A. Fernández, J. J. López-Ibor, and R. Hornero, "Changes in the MEG background activity in patients with positive symptoms of schizophrenia: spectral analysis and impact of age.," *Physiol. Meas.*, vol. 34, pp. 265–79, 2013.
- [11] N. F. Ince, G. Pellizzer, A. H. Tewfik, K. Nelson, A. Leuthold, K. McClannahan, and M. Stéphane, "Classification of schizophrenia with spectro-temporo-spatial MEG patterns in working memory," *Clin. Neurophysiol.*, vol. 120, pp. 1123–1134, 2009.
- [12] T. Xu, M. Stéphane, and K. K. Parhi, "Selection of abnormal neural oscillation patterns associated with sentence-level language disorder in Schizophrenia," in *Proceedings of the Annual International Conference of the IEEE Engineering in Medicine and Biology Society, EMBS*, 2012, pp. 4923–4926.
- [13] T. Xu, M. Stéphane, and K. K. Parhi, "Multidimensional analysis of the abnormal neural oscillations associated with lexical processing in schizophrenia.," *Clin. EEG Neurosci.*, vol. 44, pp. 135–43, 2013.
- [14] T. Xu, M. Stéphane, and K. K. Parhi, "Classification of single-trial MEG during sentence processing for automated schizophrenia screening," in *International IEEE/EMBS Conference on Neural Engineering, NER*, 2013, pp. 363–366.
- [15] M. Sabeti, S. D. Katebi, R. Boostani, and G. W. Price, "A new approach for EEG signal classification of schizophrenic and control participants," *Expert Syst. Appl.*, vol. 38, no. 3, pp. 2063–2071, 2011.
- [16] T. Harmony, T. Fernández, J. Silva, J. Bosch, P. Valdés, A. Fernández-Bouzas, L. Galán, E. Aubert, and D. Rodríguez, "Do specific EEG frequencies indicate different processes during mental calculation?," *Neurosci. Lett.*, vol. 266, pp. 25–28, 1999.
- [17] M. Stéphane, a. Leuthold, M. Kuskowski, K. McClannahan, and T. Xu, "The Temporal, Spatial, and Frequency Dimensions of Neural Oscillations Associated With Verbal Working Memory," *Clin. EEG Neurosci.*, vol. 43, pp. 145–153, 2012.
- [18] E. Bleuler, *Dementia Praecox or the Group of Schizophrenias*. New York: International Universities Press, 1950.
- [19] M. Stéphane, G. Pellizzer, C. R. Fletcher, and K. McClannahan, "Empirical evaluation of language disorder in schizophrenia.," *J. Psychiatry Neurosci.*, vol. 32, no. 4, pp. 250–258, 2007.
- [20] M. Stéphane, M. Kuskowski, and J. Gundel, "Abnormal dynamics of language in schizophrenia," *Psychiatry Res.*, vol. 216, no. 3, pp. 320–324, 2014.
- [21] R. Wix-Ramos, X. Moreno, E. Capote, G. González, E. Uribe, and A. Eblen-Zajjur, "Drug Treated Schizophrenia, Schizoaffective and Bipolar Disorder Patients Evaluated by qEEG Absolute Spectral Power and Mean Frequency Analysis.," *Clin. Psychopharmacol. Neurosci.*, vol. 12, no. 1, pp. 48–53, 2014.
- [22] J. S. Kim, K. S. Shin, W. H. Jung, S. N. Kim, J. S. Kwon, and C. K. Chung, "Power spectral aspects of the default mode network in schizophrenia: an MEG study.," *BMC Neurosci.*, vol. 15, p. 104, 2014.
- [23] J. K. Johannesen, B. F. O'Donnell, A. Shekhar, J. H. McGrew, and W. P. Hetrick, "Diagnostic specificity of neurophysiological endophenotypes in schizophrenia and bipolar disorder.," *Schizophr. Bull.*, vol. 39, no. 6, pp. 1219–29, 2013.
- [24] A. Bachiller, A. D'éz, V. Suazo, C. Domínguez, M. Ayuso, R. Hornero, J. Poza, and V. Molina, "Decreased spectral entropy modulation in patients with schizophrenia during a P300 task," *Eur. Arch. Psychiatry Clin. Neurosci.*, pp. 1–11, 2014.
- [25] Z. Zhang and K. K. Parhi, "Low-Complexity Seizure Prediction From iEEG/sEEG Using Spectral Power and Ratios of Spectral Power," *IEEE Trans. Biomed. Circuits Syst.*, vol. 10, no. 3, pp. 693–706, 2016.
- [26] Z. Zhang and K. K. Parhi, "Seizure Prediction using Polynomial SVM Classification," in *Proc. of 2015 IEEE Engineering in Medicine and Biology Society Conference (EMBC)*, 2015, pp. 5748–5751.
- [27] Z. Zhang and K. K. Parhi, "Seizure Detection using Regression Tree Based Feature Selection and Polynomial SVM Classification," in *Proc. of 2015 IEEE Engineering in Medicine and Biology Society Conference (EMBC)*, 2015, pp. 6578–6581.
- [28] R. V. A. Sheorajpanday, G. Nagels, A. J. T. M. Weeren, D. De Surgeloose, and P. P. De Deyn, "Additional value of quantitative EEG in acute anterior circulation syndrome of presumed ischemic origin," *Clin. Neurophysiol.*, vol. 121, no. 10, pp. 1719–1725, 2010.
- [29] E. Maris and R. Oostenveld, "Nonparametric statistical testing of EEG- and MEG-data," *J. Neurosci. Methods*, vol. 164, no. 1, pp. 177–190, 2007.
- [30] R. C. Oldfield, "The assessment and analysis of handedness: The Edinburgh inventory," *Neuropsychologia*, vol. 9, no. 1, pp. 97–113, 1971.
- [31] American Psychiatric Association, *Diagnostic and Statistical Manual of Mental Disorders, Fourth Edition, Text Revision*, vol. Washington, 2000.
- [32] J. R. Blair and O. Spreen, "Predicting premorbid IQ: A revision of the national adult reading test," *Clinical Neuropsychologist*, vol. 3, pp. 129–136, 1989.
- [33] J. Overall and D. Gorham, "The Brief Psychiatric Rating Scale," *Psychol. Rep.*, vol. 10, pp. 799–812, 1962.
- [34] S. R. Kay, A. Fiszbein, and L. a Opler, "The positive and negative syndrome scale (PANSS) for schizophrenia.," *Schizophr. Bull.*, vol. 13, pp. 261–76, 1987.
- [35] M. A. Gernsbacher, *Handbook of psycholinguistics*. San Diego: Academic Press, 1994.
- [36] N. Ille, P. Berg, and M. Scherg, "Artifact correction of the ongoing EEG using spatial filters based on artifact and brain signal topographies.," *J. Clin. Neurophysiol.*, vol. 19, pp. 113–124, 2002.
- [37] P. D. Welch, "The Use of Fast Fourier Transform for the Estimation of Power Spectra: A Method Based on Time Aver. aging Over Short, Modified Periodograms," *IEEE Trans. AUDIO Electroacoust.*, vol. AU-15, pp. 70–73, 1967.
- [38] K. K. Parhi and M. Ayinala, "Low-Complexity Welch Power Spectral Density Computation," *IEEE Trans. Circuits Syst. Regul. Pap.*, vol. 61, no. 1, pp. 172–182, 2014.
- [39] H. Peng, F. Long, and C. Ding, "Feature selection based on mutual information: Criteria of Max-Dependency, Max-Relevance, and Min-Redundancy," *IEEE Trans. Pattern Anal. Mach. Intell.*, vol. 27, pp. 1226–1238, 2005.
- [40] S. Mika, G. Ratsch, J. Weston, and B. Scholkopf, "Fisher discriminant analysis with kernels," *Neural Networks Signal Process. IX, 1999. Proc. 1999 IEEE Signal Process. Soc. Work.*, pp. 41–48, 1999.
- [41] Y. Freund and R. E. Schapire, "Large margin classification using the perceptron algorithm," *Mach. Learn.*, vol. 37, no. 3, pp. 277–296, 1999.
- [42] B. E. Boser, I. M. Guyon, and V. N. Vapnik, "A Training Algorithm for Optimal Margin Classifiers," in *Proceedings of the 5th Annual ACM Workshop on Computational Learning Theory*, 1992, pp. 144–152.
- [43] C. Cortes and V. Vapnik, "Support-vector networks," *Mach. Learn.*, vol. 20, no. 3, pp. 273–297, 1995.
- [44] M. Stéphane, N. F. Ince, A. Leuthold, G. Pellizzer, A. H. Tewfik, C. Surerus, M. Kuskowski, and K. McClannahan, "Temporospatial characterization of brain oscillations (TSCBO) associated with subprocesses of verbal working memory in schizophrenia.," *Clin. EEG Neurosci.*, vol. 39, no. 4, pp. 194–202, 2008.
- [45] J. P. Roiser, R. Wigton, J. M. Kilner, M. A. Mendez, N. Hon, K. J. Friston, and E. M. Joyce, "Dysconnectivity in the frontoparietal attention network in schizophrenia," *Front. Psychiatry*, vol. 4, 2013.
- [46] M. Sabeti, S. Katebi, and R. Boostani, "Entropy and complexity measures for EEG signal classification of schizophrenic and control participants," *Artif. Intell. Med.*, vol. 47, pp. 263–274, 2009.



Tingting Xu (S'13) received the B. Eng. degree in Electronic Information Engineering and the M. Eng. degree in Signal and Information Processing from Nanjing University of Posts and Telecommunications, Nanjing, China, in 2007 and 2010, respectively. She is currently working toward the Ph.D. degree in the Department of Electrical and Computer Engineering, University of Minnesota, Minneapolis, MN, USA. Her current research area includes signal and information processing, machine learning, pattern recognition, and

biomarker discovery for mental disorders.



Massoud Stephane received his MD degree from Damascus University College of Medicine in 1983. He had residency training in Neurology at the Ecole de Medicine Pitie-Salpetriere in Paris, France and in Psychiatry at Tufts University, Boston, MA and Yale University, New Haven, CT. Dr. Stephane also had a fellowship training in brain functional imaging at Johns Hopkins University, Baltimore, MD. He joined the department of psychiatry at the University of Minnesota in 1999 as an assistant professor and moved

in 2013 to the Psychiatry Department at Oregon Health and Science University where he is currently an affiliate associate Professor. Dr. Stephane is currently about to join the Department of Psychiatry at Indiana University as an associate professor. His research is focused on understanding the neural mechanisms of hallucinations as well as cognitive and linguistic impairments associated with psychosis. For this goal, Dr. Stephane employs methodologies based on the phenomenology of the disease, cognitive modeling and brain imaging with magnetoencephalography and fMRI.



Keshab K. Parhi (S'85-M'88-SM'91-F'96) received the B.Tech. degree from IIT Kharagpur, Kharagpur, India, in 1982, the M.S.E.E. degree from the University of Pennsylvania, Philadelphia, PA, USA, in 1984, and the Ph.D. degree from the University of California at Berkeley, Berkeley, CA, USA, in 1988. He has been with the University of Minnesota, Minneapolis, MN, USA, since 1988, where he is currently a Distinguished Mc Knight University Professor and an Edgar F. Johnson Professor with the Department of Electrical and Computer Engineering. He has published over 575

papers, is the inventor or co-inventor of 29 patents, has authored the textbook VLSI Digital Signal Processing Systems (New York, NY, USA: Wiley, 1999), and co-edited the reference book Digital Signal Processing for Multimedia Systems (Boca Raton, FL, USA: CRC Press, 1999). His current research interests include the VLSI architecture design and implementation of signal processing, communications and biomedical systems, error control coders and cryptography architectures, high-speed transceivers, stochastic computing, secure computing, and molecular computing. He is also currently working on intelligent classification of biomedical signals and images, for applications such as seizure prediction and detection, schizophrenia classification, biomarkers for mental disorders, brain connectivity, and diabetic retinopathy screening.

Dr. Parhi has served on the Editorial Boards of the IEEE TRANSACTIONS ON CIRCUITS AND SYSTEMS PART I AND PART II, VLSI Systems, Signal Processing, the IEEE SIGNAL PROCESSING LETTERS, and the IEEE SIGNAL PROCESSING MAGAZINE, and served as the Editor-in-Chief of the IEEE TRANSACTIONS ON CIRCUITS AND SYSTEMS PART I from 2004 to 2005. He currently serves on the Editorial Board of the Springer Journal of Signal Processing Systems. He has served as the Technical Program Co-Chair of the 1995 IEEE VLSI Signal Processing Workshop and the 1996 Application Specific Systems, Architectures, and Processors Conference, and as the General Chair of the 2002 IEEE Workshop on Signal Processing Systems. He was a Distinguished Lecturer of the IEEE Circuits and Systems Society from 1996 to 1998. He served as a Board of Governors Elected Member of the IEEE Circuits and Systems Society from 2005 to 2007. He is a recipient of numerous awards, including the 2013 Distinguished Alumnus Award from IIT Kharagpur, the 2013 Graduate/Professional Teaching Award from the University of Minnesota, the 2012 Charles A. Desoer Technical Achievement Award from the IEEE Circuits and Systems Society, the 2004 F. E. Terman Award from the American Society of Engineering Education, the 2003 IEEE Kiyo Tomiyasu Technical Field Award, the 2001 IEEE W. R. G. Baker Prize Paper Award, and the Golden Jubilee Medal from the IEEE Circuits and Systems Society in 2000.